Single Event Upsets and Hot Pixels in Digital Imagers

Glenn H. Chapman, Rahul Thomas, Rohan Thomas, Klinsmann J. Coelho Silva Meneses, Tommy Q. Yang
School of Engineering Science
Simon Fraser University
Burnaby, B.C., Canada, V5A 1S6
glennc@ensc.sfu.ca, rmt3@sfu.ca, rohant@sfu.ca, klinsmannjoel@hotmail.com, tqyang@sfu.ca

Israel Koren, Zahava Koren
Dept. of Electrical and Computer Engineering
University of Massachusetts
Amherst, MA, 01003
koren,zkoren@ecs.umass.edu

***Abstract*— From extensive study of digital imager defects, we found that permanent "Hot Pixels" are the main long term digital camera defects, and are caused by high energy cosmic ray particles. Clearly, as in other microelectronic integrated circuits, most of the particles do not induce permanent damage but instead, inject a short term charge that may cause a transient fault, known as a Single Event Upset (SEU). Unlike standard digital ICs, pixels in a digital imaging sensor can be monitored at almost any desirable frequency. Since an SEU manifests itself as one or more brighter pixels in an otherwise dark image, the rate of SEUs can be measured at a considerably higher accuracy by taking dark-field pictures at different exposure times and different frequencies. In this paper we describe an experimental approach to measuring the occurrence rate and resulting characteristics of SEUs. The SEU rate that we have observed for digital imagers, of about 4 SEUs for every 30 seconds, is considerably higher than was previously reported for ordinary ICs. For the same imager, permanent hot pixels have a rate of 1 every 12.6 days, while SEUs occur 145,000 times more often. Ordinary IC SEU rates have been reported to be about 100× of permanent fault rates. In addition, we found that some SEUs in digital imagers do not impact a single pixel, as do hot pixels, but can create a line of injected charges which appears as a bright line in the dark image.**

Keywords- imager defects, hot pixel, SEU, active pixel sensor, APS, CCD, ISO

I. Introduction

In today's world of photography, digital imagers and their associated technology have become a central theme of development and innovation. Modern day cell phones and embedded sensors in cars all have integrated digital imagers. Their uses range from medical to industrial and scientific applications, and are increasing in many engineering solutions. The increased demand for digital imagers creates an inherent drive and push for enhanced sensors via a decrease in pixel size and an increase in imager sensitivity. Given that digital imager sensors are microelectronic in nature, they are susceptible, like other integrated circuits, to developing defects over time. These defects can be permanent, appearing soon after fabrication and increasing in number during the lifetime of the sensor. Such defects degrade image quality, especially in applications where image accuracy and pixel sensitivity are key.

Over the past several years, our research was focused mainly on the analysis of in-field permanent defects; their development, their characterization, and their growth rate [1-6]. This type of defect is known as a 'Hot Pixel.' These studies have resulted in an empirical formula, which projects that as the pixel size shrinks and the sensitivity increases, defect numbers will grow via a power law. It also suggests that as pixel sizes decrease to less than two microns, and sensitivities move towards allowing low light night pictures, defect rates can grow to hundreds or even thousands per year. The defect growth rate is modeled as a function of pixel size, sensor area and ISO. Previous research has shown that that in-field defects are likely the result of cosmic ray damage [1-3].

Similarly to other ICs, imagers are also subject to transient defects. These are defects that are seen in-field but are short-lived and therefore appear in only a single image. In this paper we discuss the nature of Single Event Upsets (SEUs) as they apply to imagers. SEUs are caused by cosmic particles that strike the imager at random times and locations. Depending on the particle energy, the SEU can cause a soft error than can be noticed in the actual values collected by a pixel. In the literature there has been considerable study of SEUs as they relate to digital ICs [10,11]. More recent research has started to look at SEUs in digital imagers, including the use of cell phone sensors as detectors for cosmic ray activity [12]. In digital ICs it is known that SEUs occur typically at about 100 times greater rate than permanent faults. However, the SEU rate (or number of temporarily erroneous pixels) as compared to the rate of permanent hot pixels in digital imagers has not been discussed. This is important as it helps understand the effect of these temporary defects at different ISO/exposure times and also enables camera manufacturers to better design for reliability and fault tolerance. Therefore, the understanding of image sensor behavior in the presence of SEUs is vital.

This paper is organized as follows: Section II summarizes the classical model of imager *hot pixels* and their growth rate. Section III describes the experimental method we used to collect the SEU data in imagers, and Section IV discusses the numerical results of our experiments. Section V shows the analysis of our experimental results. Finally, Section VI concludes the paper.

II. HOT PIXELS

Over the past 10 years [5,6], we have been studying the characteristics of imager defects by manually calibrating many commercial cameras ranging from small cell phone to Digital Single Lens Reflex (DSLRs), by taking exposures of dark fields (i.e., no illumination). This helps us to identify stuck-high and partially stuck defects. Up till now, we have not identified any stuck high pixel types in our experiments. Instead, the prominent defect type is called hot pixels. The

978-1-4799-8606-4/15/$31.00

standard hot pixel has a dark response that has an illumination-independent component that increases linearly with exposure time, and can, therefore, be identified by capturing a series of dark field images at increasing exposure times. Figure 1 displays the dark response of a hot pixel, showing the normalized pixel illumination versus the exposure time, where illumination level 0 represents no illumination and level 1 represents saturation. Three different pixel responses are shown in Figure 1. Firstly a good pixel is displayed as curve Fig.1(a). Since there is no illumination, we expect the pixel output to be constantly zero for all exposures. The other two curves depict the two different types of hot pixels [5]. Curve Fig. 1(b) is a standard hot pixel which has an illumination-independent component that increases linearly with exposure time. The third response shown as curve Fig. 1(c) is a partially stuck hot pixel which has an additional offset that manifests even at no exposure.

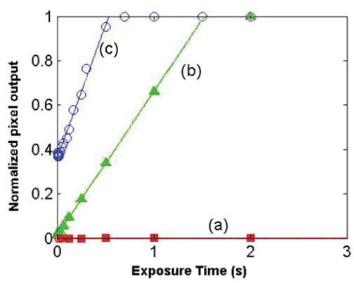

Figure 1: Comparing the dark response of imager pixels (a) good pixel, (b) standard hot pixel, (c) hot pixel with offset.

Although imagers are generally referred to as digital systems, the actual pixel sensor is an analog device. The classic assumed response of good and hot pixels to illumination can be modeled using Equation (1), where I_{pix} is the response, R_{photo} measures the incident illumination rate, R_{dark} is the dark current rate, T_e measures of the exposure time, b is the dark offset, and m is the amplification due to the ISO setting.

$$I_{pix}(R_{photo}, R_{dark}, T_e, b) = m*(R_{photo}\ T_e + R_{dark}\ T_e + b) \qquad (1)$$

For a good pixel, both R_{dark} and b are zero, resulting in the output response being a direct measure of the incident illumination. However, for the case of hot pixels, these two terms create a signal that is added onto the incident illumination, and therefore the pixel output appears to be brighter. To estimate the dark response of a pixel, I_{offset}, can be found by setting R_{photo} to zero which yields

$$I_{offset}(R_{dark}, T_e, b) = m*(R_{dark} T_e + b) \qquad (2)$$

The dark response equation in Equation (2), sometimes called the combined dark offset, is linear. Thus, the parameters R_{dark} and b can be extracted by fitting the pixel response in a dark frame vs. exposure time, as seen in Figure 1. For standard hot pixels, b is zero. These hot pixels are most visible in longer exposures as they do not have an initial offset. In the partially stuck hot pixel case, the magnitude of b affects the response. This defect will appear in all images. Obtaining this data for each camera involves typically 5 to 20 calibration images per test at a wide range of exposure times and ISO's, and their analysis with specialized software [2-4].

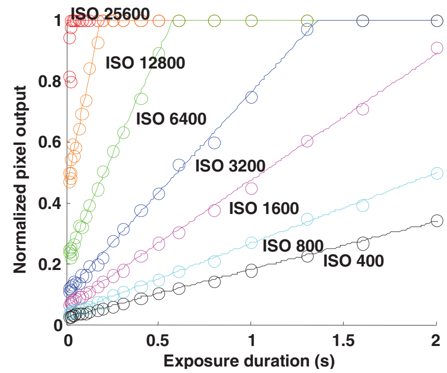

Figure 2: Dark response of a hot pixel at various ISO levels

Figure 2 shows the dark response of a hot pixel that we have measured for varying ISO levels. For low ISO, defects have low values of R_{dark} and b. Both R_{dark} and b increase dramatically, as the ISO amplification increases, scaling linearly with the ISO (see Equation (1)). In fact, at ISO 12800, the dynamic range of the pixel is reduced by 40% solely due to the offset b, and at ISO 25600 the pixel is near saturation at all exposures. The high number of hot pixels with offsets suggests that the development of stuck high pixels in the field may actually be due to the presence of hot pixels with very high offsets. This is consistent with our experience of not having detected a true stuck pixel in any of our cameras, while explaining the cameras developing stuck pixels discussed in camera forums.

Studying both the spatial and temporal growth of hot pixels, we have concluded that they occur randomly over the imager [1-6], indicating a source that is also random in nature, most likely cosmic rays. These results have also been observed by other authors, who have shown that neutrons seem to create the same hot pixel defect types [7, 8]. We recently developed, in [9], an empirical formula to relate the defect density D (defects per year per mm^2 of sensor area) to the pixel size S (in microns) and sensor gain (ISO) via the following equations:

For APS pixels: $D=10^{-1.13}\ S^{-3.05} ISO^{0.505}$ (3)

For CCD sensors $D=10^{-1.849}\ S^{-2.25} ISO^{0.687}$ (4)

These equations show us that the defect rate increases drastically when the pixel size falls below 2 microns, and is projected to reach 12.5 defects/year/mm^2 at ISO 25,600 (which is already available on some high-end cameras).

Clearly, digital imagers suffer transient faults in addition to the permanent hot pixel defects, and our current research efforts are focused on finding, identifying and analyzing these SEUs in digital imagers.

III. EXPERIMENTAL SETUP

In order to identify SEUs, we used DSLRs as our first test devices because they have large imager areas with highly sensitive pixels, and allow direct access to the pixel RAW values without image processing such as jpeg that tends to distort the data [4]. The experimental method for this research differs than what we used in the hot pixel research. For the hot pixel experiments, a series of images were taken at increasing exposure times with a fixed ISO. Then a linear fit was performed in order to create a curve as shown in Figure 2. However, for the SEU experiments we took a series of medium to long exposures at a fixed ISO. Because the exposure time for each image is fixed, this allows us to look for events the only occur in a single image and then go away. The key point is that SEUs are by their nature very short in duration and suddenly inject a charge into the local area of the IC. However, in digital imagers the pixel integrates charge changes over the duration of the exposure, and by taking an exposure of a given duration the imager records both the temporal and spatial occurrence of each SEU even if the SEU disappears. Still, we could not take very long exposures with digital cameras as they accumulate noise in the image (e.g., thermal generated electrons) over time. The maximum exposure time varies with the camera and the ISO but is typically in the order of 10 to 30 seconds before noise becomes so prevalent that identifying SEUs is difficult. Hence, in our experiments we needed to take a sequence of short duration images.

In order to effectively measure the effect of SEUs on imagers for various operating conditions, we created an experimental setup to collect a large number of dark-frame images. Effectively, these images needed to be precise temporal snapshots of the sensor activity for a specific time period at given various camera settings: ISO levels and exposure times. The sequence of images also allows us to separate SEUs from the hot pixel events and obtain a temporal rate for these short duration events.

In designing the experiments we first used a camera with a large imager (36 by 24 mm^2) and a high sensitivity (ISO) which previous research showed would develop about one hot pixel every 12.5 days. Based on the reported ratio of 100 SEUs for each permanent fault, we expected to have to take a large number of pictures before detecting a noticeable number of events. In practice it turned out that SEUs were more common than we expected, and our setup resulted in a significant number of detections.

In order to take multiple shots at a fixed ISO and exposure time, we made use of a digital camera remote control, called an intervelometer, which would take a set sequence of images. The remote was set up such that after each shot (image), a one minute delay was inserted to remove any effects of thermal noise caused by the sensor heating up as the experiment progressed. On average, a set of 100 images was collected for each ISO and exposure time combination. The 100 image number was also set by the maximum picture limit of the camera batteries.

It is important to note that these experiments were all conducted in a pitch dark room so that no incident light fell onto the camera sensor. This enabled us to detect any temporary defects caused by SEUs.

To analyze the images for SEU artifacts, a software tool was created. This tool read in the RAW images and executed the following algorithm using 3 consecutive images at a time:

- Flag any pixels that have a pixel increase from image j to image j+1 using a predetermined threshold
- Using the pixel locations from the previous step, check to see if any of them have a decrease in pixel values from image j+1 to image j+2 using the same predetermined threshold
- If any pixel location satisfies the above conditions, it is marked as an SEU defect location

This algorithm can be clearly seen in Figure 3. One thing to note is that our algorithm ignores locations where known hot pixels resided. Given our previous research with hot pixels on this particular imager, the hot pixel locations were known and were not used in the analysis in order to avoid any false positive results.

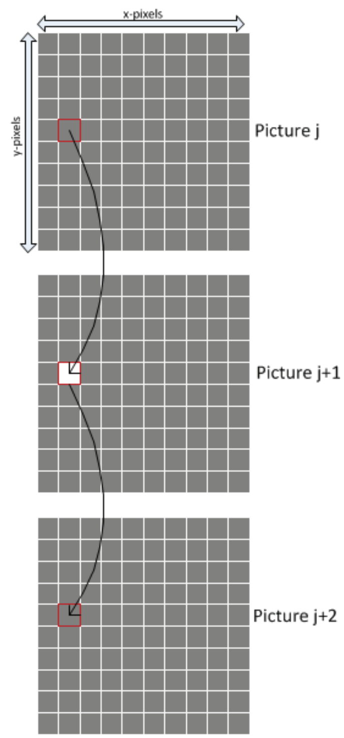

Figure 3: SEU Detection Algorithm demonstrating an SEU that was detected in image 'j+1' and not present in images 'j' and 'j+2'

IV. EXPERIMENTAL RESULTS

Using the SEU detection algorithm mentioned in the previous section, we conducted experiments at different ISO and exposure levels to collect SEU defect counts. One important thing to note is that the camera that was used for this experiment was set-up such that no image post-processing was introduced (i.e. RAW images were used). RAW images are the minimally processed pictures that essentially contain pixel data as taken by the camera. There are no processing algorithms or demosaicing performed on the RAW images.

As a starting point we began at ISO 6400, performing experiments at 30s, 10s, 3.2s and 1s. For each experiment about 100 images were taken. During our first set of experiments, we have discovered several interesting forms of SEU defects, specifically SEU streaks. An example is shown in Figure 4. In this example, an incident cosmic ray has hit the imager at a low angle, depositing a charge covering 3 neighboring pixels in a line. We consider this a single particle hit as the cause of this streak is likely a single SEU. We justify this by noting that the event rate (at most a few SEUs per a 21 megapixel image) is such that the probability of 3 events occurring as neighbors is extremely low. Moreover, such streaks turned out to be a common occurrence. These streaks are really the charge equivalent of the trails left by cosmic ray particles in the classic cloud chamber detectors.

Figure 4: Simple SEU Streak (snapshot of 5x5 pixels in size)

A more complicated streak is shown in Figure 5. In this example, it is clear that the incident cosmic particle began at a particular direction. However, at some point, it incurred a deflection. One possibility is that the incident cosmic ray particle collided with an atom, causing the particle to deflect and creating this interesting SEU defect. From the figure it is clear that there are gaps in the streak which are likely due to some pixels not accumulating enough charge from the incident particle to show the SEU brightness.

With this complex observation of streaks with inherent gaps, we upgraded our algorithm to consider a streak as a single SEU hit. This method also took into account streaks that had gaps. This enables us to effectively treat an SEU that created a multiple streak as one single event. Such a streak is shown in Figure 6 in which the streak circled in red is considered as a single SEU hit. The figure also shows a simple SEU defect that is only detected at a single pixel spot

V. Analysis of Results

Using the data obtained by our experiments we can now attempt to define certain trends and rates of SEU growth at various operating conditions of the imager. We have counted SEUs that appear in streaks as a single defect as shown in Figure 6. Figures 7 – 10 display the defect count distribution for each exposure time for the ISO 6400 experiments. In all of the distributions shown,

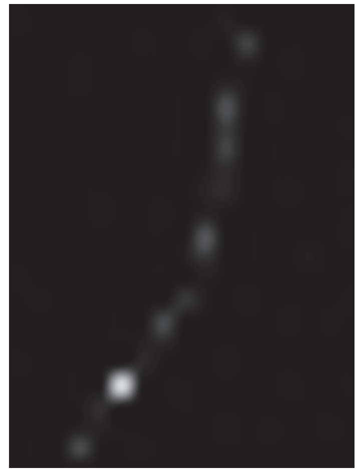

Figure 5: Complex SEU Streak (snapshot of 12x17 pixels in size)

These results indicate, as is expected, that the defect rate increases as the exposure time increases. For radiation type events, a common assumption is that their number follows a Poisson process as shown in Equation 5, where **λ** is the event rate (per second) and λt is the expected value of the number of events occurring in t seconds.

$$f(k,\lambda,t) = \frac{(\lambda t)^k e^{-\lambda t}}{k!} \tag{5}$$

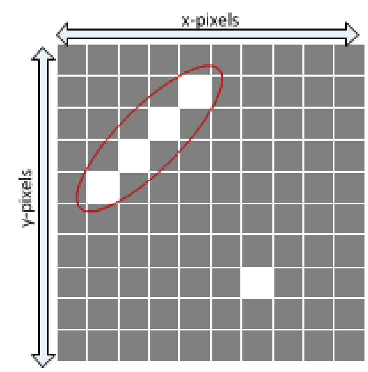

Figure 6: SEU types – simple SEU spot (bottom) and SEU cluster (top)

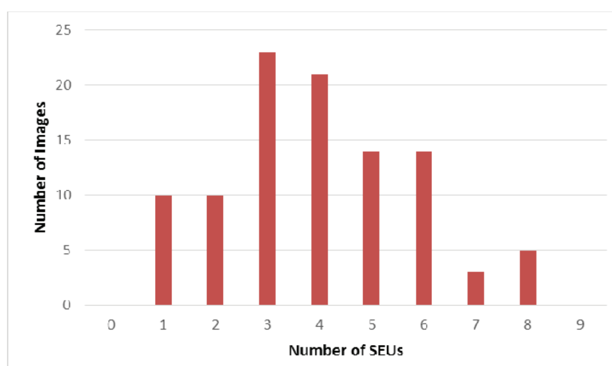

Figure 7: Distribution of number of SEUs per image
(ISO 6400, t=30s)

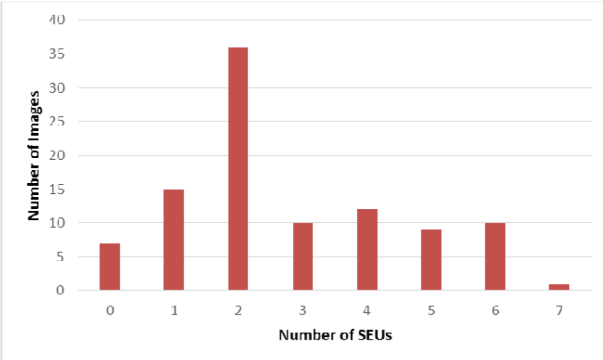

Figure 8: Distribution of number of SEUs per image
(ISO 6400, t=10s)

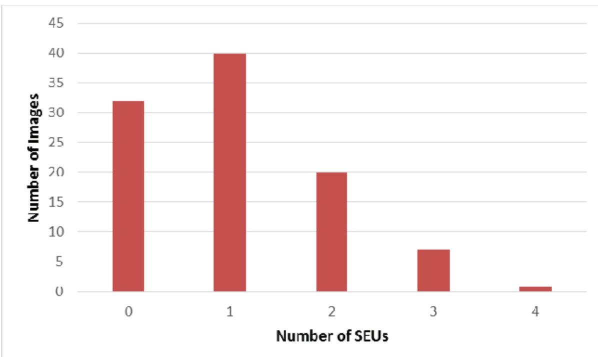

Figure 9: Distribution of number of SEUs per image
(ISO 6400, t=3.2s)

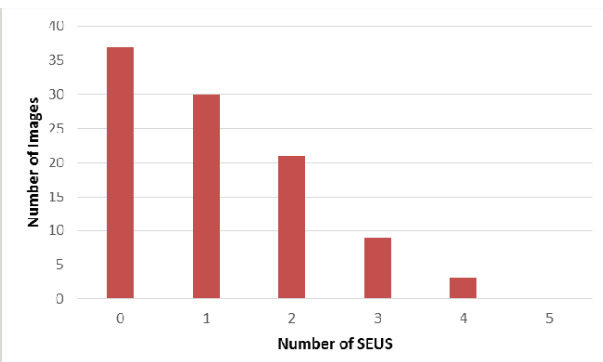

Figure 10: Distribution of number of SEUs per image
(ISO 6400, t=1s)

For each value of t, we estimated the expected value λt. Figure 11 plots λt for ISO 6400 and ISO 1600 over a range of exposure lengths t. Note that in this plot the exposure time is in log scale.

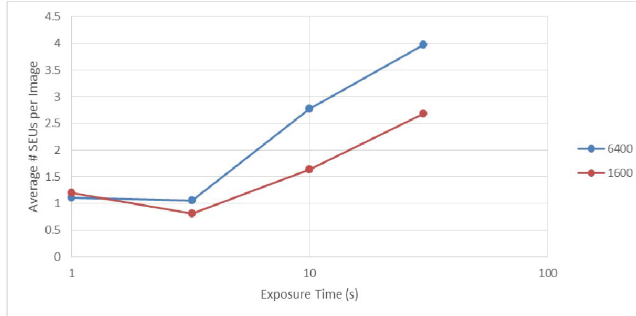

Figure 11 Average number of SEUs per image vs exposure time
for 1600 and 6400ISO settings (log scale)

Figure 11 suggests that SEU defect rates increase with ISO. However, this increase is not constant over exposure times. It is clear that for larger exposure times, the increase is greater (with a slope of approximately 0.069 SEUs/second), while for smaller exposure times the difference is much smaller. Also, note that there is a drop in the defect count below the 3.2s exposures for both ISO 1600 and ISO 6400. Though not fully understood at this point, it should be noted that the camera performs some level of background dark frame subtraction around the 1s exposure point. For exposures greater than about 1 s, the camera takes its own dark field image in addition to the exposed image, which is then subtracted from the original data to reduce noise in the image. This subtraction threshold possibly produces the sudden change in the curves at this point

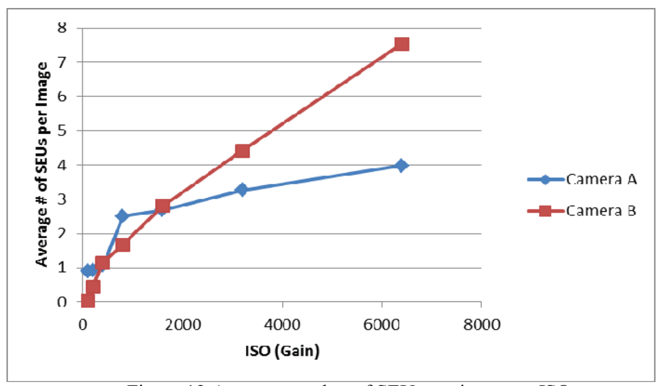

Figure 12 Average number of SEUs per image vs ISO
(for a 30s exposure) for 2 cameras scaled to camera A (36x24mm)

To further illustrate the effects of ISO on the defect rate, we plotted the averages λt for ISO 100, 200, 400, 800, 1600, 3200 and 6400 as shown in Figure 12 for two different imagers. For each ISO, the exposure time was fixed at t=30s. It is clear that the defect rate increases with ISO. For camera A from ISO 800 onwards the defect rate grows linearly with ISO at $0.26\text{x}10^{-3}$ SEU/ISO. At ISO 400 and lower ISOs the rate suddenly falls showing the gain is too small for many SEU's to be seen above the noise Threshold. An interesting point is that the 400 ISO images do not show the streaks that are seen at higher ISOs. This suggests that there may be several different causes of SEUs (i.e., different cosmic ray particles types creating different effects). The streaks are lower energy events and are therefore not evident in the lower ISOs. Camera B shows a similar behavior, but the linear region starts at 400 ISO, and the slope is 1.01×10^{-3} SEU/ISO or 4.3x steeper. This may reflect the camera differences, of larger sensor area and smaller pixels (see Table 1). This plot scales the rate to the Camera A sensor size.

One question that we have not answered yet is what the exact cause is for SEUs in digital imagers. Traditional studies point towards neutron particles being the primary cause [10]. Another belief is that muons are the source of these soft errors [11]. Though a definite answer is yet to be determined, the trend in Figure 12 suggests that a combination of neutrons and muons causes these SEU defects. Firstly, at low ISOs we see that almost all defects are single spots and not the clustered kind. Additionally, the number of clusters increases as the ISO increases. Other researchers have identified streaks in imagers as being caused by cosmic ray generated muons, which are lower energy events than the cosmic ray neutrons [12]. This leads us to believe that muons are the probable cause of streak defects, while neutrons more likely generate single pixel defects (similarly to what is seen in digital IC circuits).

Table 1 SEU Defect Rates for 3 APS Digital Imagers (t=10s, ISO 1600)

Camera	λt	$\lambda t\,/cm^2$	Sensor Size (mm × mm)	Pixel (µm)
A	1.640	0.189	36.0 × 24.0	6.26
B	0.481	0.145	22.3 × 14.9	4.30
C	0.654	0.190	22.7 × 15.1	7.38

To confirm that similar behavior is observed across different imagers, we have performed tests on two additional cameras at ISO 1600 with a $t=10s$ exposure time as shown in Table 1 (A is the camera used in the previous sections). All the imagers in this table have APS sensors and the experiments were conducted and analyzed using the same methodology. For all three cameras, the average number of defects λt was extracted. However, each camera has a different sensor size which means that the λt values cannot be directly compared, but have to be scaled by the sensor area of the camera.

The results of Table 1 tell us some important points. Firstly, SEUs are not limited to one imager but are observable in multiple imagers, making the research repeatable. Secondly, the rates of SEU defects for each camera are fairly consistent. Cameras A and C have higher rates that are quite close to each other. It should be noted that Camera B has smaller pixels (4 µm compared to 7) which may indicate that pixel size has an impact on the SEU rate. Though Camera B has a smaller rate at ISO 1600, at higher ISOs it is observed that the rate can increase to greater than that of Camera A.

The SEU rate that we have observed for digital imagers, of about 4 SEUs for every 30 seconds, is considerably higher than was previously reported for ordinary ICs. Permanent hot pixels for the same imager have a rate of about 1 every 12.6 days by our previous measurements [6], so SEUs are 145,000 times more common. By comparison, for ordinary ICs the literature indicates that SEUs are about 100 times more common than permanent faults. This much higher rate in digital imagers is most likely the result of the much higher sensitivity of pixels to injected charges. However, as Figure 12 suggests, it may also be that imager SEU's are detecting other cosmic ray events, such as muons, that do not affect other digital circuits. Table 1 also suggests the important area that we do not yet have enough data to explore. In the case of hot pixels we saw a strong power law relationship between the pixel size and the hot pixel development rate. We need to see how the hot pixel rate versus SEU rate changes as a function of pixel size.

VI. Conclusions

This paper has demonstrated that SEUs occur much more often in digital imagers than in regular ICs, and obviously, more often than permanent hot pixels. As SEUs are easily detectable in digital imagers, we plan on further studying their rates as a function of the amplitude (the amount of charge injected by the particle hit). Such a study can prove to be useful for SEUs in regular ICs as well. Further research will determine how the ratio between the SEU rate and hot pixel rate varies with the imager parameters.

References

[1] J. Dudas, L.M. Wu, C. Jung, G.H. Chapman, Z. Koren, and I. Koren, "Identification of in-field defect development in digital image sensors," *Proc. Electronic Imaging, Digital Photography III*, v6502, 65020Y1-0Y12, San Jose, Jan 2007.

[2] J. Leung, G.H. Chapman, I. Koren, and Z. Koren, "Statistical Identification and Analysis of Defect Development in Digital Imagers," *Proc. SPIE Electronic Imaging, Digital Photography V*, v7250, 742903-1 – 03-12, San Jose, Jan 2009.

[3] J. Leung, G. Chapman, I. Koren, and Z. Koren, "Automatic Detection of In-field Defect Growth in Image Sensors," *Proc. of the 2008 IEEE Intern. Symposium on Defect and Fault Tolerance in VLSI Systems*, 220-228, Boston, MA, Oct. 2008.

[4] J. Leung, G. H. Chapman, I. Koren, Z. Koren, "Tradeoffs in imager design with respect to pixel defect rates," *Proc. of the 2010 Intern. Symposium on Defect and Fault Tolerance in VLSI*, 231-239., Kyoto, Japan, Oct 2010.

[5] J. Leung, J. Dudas, G. H. Chapman, I. Koren, Z. Koren, "Quantitative Analysis of In-Field Defects in Image Sensor Arrays," *Proc. 2007 Intern. Sym on Defect and Fault Tolerance in VLSI*, 526-534, Rome, Italy, Sept 2007.

[6] J. Leung, G.H. Chapman, Y.H. Choi, R. Thomson, I. Koren, and Z. Koren, "Tradeoffs in imager design parameters for sensor reliability," Proc., *Electronic Imaging, Sensors, Cameras, and Systems for Industrial/Scientific Applications XI*, v 7875, 78750I1-0I12, San Jose, Jan. 2011.

[7] A.J.P. Theuwissen, "Influence of terrestrial cosmic rays on the reliability of CCD image sensors. Part 1: experiments at room temperature," *IEEE Transactions on Electron Devices*, Vol. 54 (12), 3260-6, 2007.

[8] A.J.P. Theuwissen, "Influence of terrestrial cosmic rays on the reliability of CCD image sensors. Part 2: experiments at elevated temperature," *IEEE Transactions on Electron Devices*, Vol. 55 (9), 2324-8, 2008.

[9] G.H. Chapman, R. Thomas, I. Koren, and Z. Koren, "Empirical formula for rates of hot pixel defects based on pixel size, sensor area and ISO", *Proc. Electronic Imaging, Sensors, Cameras, and Systems for Industrial/Scientific Applications XIII*, v8659, 86590C-1-C-11 San Francisco, Jan. 2013.

[10] R. Heald, 'How Cosmic Rays Cause Computer Downtime', IEEE Rel. Soc. SCV Meeting, 2005.

[11] Wipac.wisc.edu, 'Deco'. [Online]. Available: http://wipac.wisc.edu/deco. [Accessed: 15- May- 2015].

[12] Kurzweilai.net, 'How to turn your Android phone into a cosmic ray detector', 2014. [Online]. Available: http://www.kurzweilai.net/how-to-turn-your-android-phone-into-a-cosmic-ray-detector. [Accessed: 15- May- 2015].